Climate Dynamics (2005)
DOI 10.1007/s00382-005-0059-7

B. Decharme · H. Douville

Introduction of a sub-grid hydrology in the ISBA land surface model

Received: 31 March 2005 / Accepted: 12 July 2005

Abstract In atmospheric models, the partitioning of precipitation between infiltration and runoff has a major influence on the terrestrial water budget, and thereby on the simulated weather or climate. River routing models are now available to convert the simulated runoff into river discharge, offering a good opportunity to validate land surface models at the regional scale. However, given the low resolution of global atmospheric models, the quality of the hydrological simulations is much dependent on various processes occurring on unresolved spatial scales. This paper focuses on the parameterization of sub-grid hydrological processes within the ISBA land surface model. Five off-line simulations are performed over the French Rhône river basin, including various sets of parameterizations related to the sub-grid variability of topography, precipitation, maximum infiltration capacity and land surface properties. Parallel experiments are conducted at a high (8 km by 8 km) and low (1° by 1°) resolution, in order to test the robustness of the simulated water budget. Additional simulations are performed using the whole package of sub-grid parameterizations plus an exponential profile with depth of saturated hydraulic conductivity, in order to investigate the interaction between the vertical soil physics and the horizontal heterogeneities. All simulations are validated against a dense network of gauging measurements, after the simulated runoff is converted into discharge using the MODCOU river routing model. Generally speaking, the new version of ISBA, with both the sub-grid hydrology and the modified hydraulic conductivity, shows a better simulation of river discharge, as well as a weaker sensitivity to model resolution. The positive impact of each individual sub-grid parameterization on the simulated discharges is more obvious at the low resolution, whereas the high-resolution simulations are more sensitive to the exponential profile with depth of saturated hydraulic conductivity.

B. Decharme (✉) · H. Douville
Météo-France, CNRM/GMGEC/UDC, 42 ave. G. Coriolis, 31057 Toulouse Cedex1, France
E-mail: bertrand.decharme@cnrm.meteo.fr
Fax: +33-561-07-9610

1 Introduction

Over recent years, more and more attention has been paid to the partitioning of precipitation between infiltration and runoff in both meteorological and climate models. Indeed, the simulated land surface water budget has been shown to have a strong impact on the overlying atmosphere on a wide range of space and time scales. For example, an increasing number of studies based on atmospheric general circulation models (AGCMs) suggest that soil wetness exerts a significant influence on both climate variability and predictability (see Douville 2003 for a brief review). Unfortunately, soil wetness is still unknown over most of the globe because in situ measurements are very sparse, and remote sensing techniques are only partially effective. As a consequence, river routing models are now frequently used to convert runoff into river discharge, and thereby to validate the land surface water budget simulated in climate models over large river basins (Douville et al. 2002; Ducharne et al. 2003).

The space–time variability of the land surface processes is usually represented in AGCMs through the use of land surface models (LSMs). The complexity of these models ranges from the simple bucket model (Manabe 1969) to more sophisticated soil–vegetation–atmosphere transfer schemes with multiple parameterizations representing the physical processes linked to vegetation, soil and snow. Although these models have been significantly improved over recent decades, hydrological applications still remain a challenge for state-of-the-art LSMs. The simulated runoff is extremely dependent on the model physics and must be carefully validated if one wants to predict not only precipitation, but also river discharge on various time scales (from short-range

forecasts to multi-decadal climate scenarios). The coupling of LSMs with river routing models appears as a powerful tool for understanding the regional and global water cycles (Dümenil and Todini 1992; Habets et al. 1999b; Oki et al. 1999; Etchevers et al. 2001), predicting streamflow (Habets et al. 2004), and improving SVAT parameterizations (Lohmann et al. 1998; Wood et al. 1998; Chapelon et al. 2002; Boone et al. 2004; Decharme et al. 2005).

In global AGCMs, the land surface water budget is calculated on grid cells whose side measures typically from 50 km to 300 km. With such a resolution, the quality of the hydrological simulations is very dependent on various processes occurring on unresolved spatial scales. Consequently, the precipitation and land surface heterogeneities within a grid box are of primary importance for the simulated surface hydrology. For LSMs applied at regional to global scales, the relevance of sub-grid variability has been shown in several LSM intercomparison projects where LSMs have been used in off-line mode (driven using prescribed atmospheric forcing) and the resulting simulations have been compared to observations (Lohmann et al. 1998; Wood et al. 1998; Dirmeyer 1999; Boone et al. 2004).

A general conclusion of the Phase-1 of the Global Soil Wetness Project (Dirmeyer 1999; http://www.iges.org/gswp/) is that parameterization of sub-grid heterogeneity, either through an explicit modeling of tiles or a statistical approach, is useful to properly partition precipitation between total runoff and evapotranspiration. Another contribution to the understanding of the scaling influence on LSMs was made by the Rhône-Aggregation (Rhône-AGG) project (http://www.cnrm.meteo.fr/mc2/projects/rhoneagg/), which was recently undertaken at Météo-France (Boone et al. 2004). Rhône-AGG includes a broader investigation of the impact of aggregation on hydrological simulation. The first goal of Rhône-AGG was to investigate how different LSMs simulate the river water balance at high resolution for several annual cycles compared to observed data from a dense network of gauging stations. It was shown that the sub-grid runoff formulation is particularly important for simulating realistic daily discharges over the Rhône river basin. The second goal of the project was to examine the impact of changing the horizontal resolution on the simulations. Results from a series of scaling experiments were examined in which the spatial resolution was decreased to be more consistent with that of AGCMs. The general conclusion was that LSMs that take account of land surface and/or atmospheric forcing spatial heterogeneities are able to reduce the scaling influence on the simulated water budget.

The present study describes a new set of parameterizations of sub-grid hydrological processes within the ISBA LSM for use in regional and global applications. These parameterizations represent the spatial variability within a grid box of topography, precipitation, maximum infiltration capacity, soil and vegetation properties, and their impact on the simulated land surface water budget. The validation of these parameterizations is conducted over the Rhône basin using the Rhône-AGG data set. The original ISBA LSM is described in Sect. 2. The new representation of land surface heterogeneities within ISBA is presented in Sect. 3. Section 4 describes the experimental design and the Rhône-AGG data set. Five simulations, including various sub-grid parameterizations within the ISBA LSM, are implemented at high and low resolutions. The main results are presented in Sect. 5. Finally, discussion and conclusions are provided in Sects. 6 and 7, respectively.

2 The ISBA land surface model

The ISBA LSM contains the basic physics of the land surface. The model is relatively simple and needs only a limited number of parameters, which depend on the type of soil and vegetation (Noilhan and Planton 1989). It uses the force-restore method (Deardorff 1977, 1978) to calculate the time evolution of the surface and mean soil temperature. The water budget is based on a soil hydrology, a rainfall interception scheme (Noilhan and Mahfouf 1996), and a one-layer snow scheme (Douville et al. 1995). The model also simulates freezing and thawing in the two uppermost layers (Boone et al. 2000).

The original ISBA LSM had only a two-layer soil hydrology: a thin surface layer with a uniform depth, d_1 (m), included in the total soil layer. More recently, a third layer was introduced by Boone et al. (1999) in order to distinguish between the rooting depth, d_2 (m), and the total soil depth, d_3 (m). In other words, the ISBA LSM now has a tree-layer soil hydrology: the root zone layer overlaps the surface layer, whereas the deep-soil reservoir extends from the base of the root zone to the base of the modeled soil column. The governing equations for the time (t) evolution of soil moisture for each layer are written as:

$$\frac{\partial w_1}{\partial t} = \frac{C_1}{\rho_w d_1}(I_r - E_{soil}) - D_1 - \frac{F_{1w}}{\rho_w d_1} \quad (1)$$

$$\frac{\partial w_2}{\partial t} = \frac{1}{\rho_w d_2}\left(I_r - E_{soil} - E_{transp}\right) - K_2 - D_2 - \frac{F_{2w}}{\rho_w d_2} \quad (2)$$

$$\frac{\partial w_3}{\partial t} = \frac{d_2}{(d_3 - d_2)}(K_2 + D_2) - K_3 \quad (3)$$

where w_1, w_2 and w_3 represent the layer-average volumetric water contents ($m^3\ m^{-3}$) for the surface, root zone, and deep soil layers, respectively. The volumetric water content within each reservoir is constrained to be less than the soil porosity or saturation water content, w_{sat} ($m^3\ m^{-3}$). F_{1w} and F_{2w} are the surface and sub-soil net phase changes, which represent mass fluxes ($kg\ m^{-2}\ s^{-1}$) from either soil ice production or melt. K (s^{-1}) represents gravitational drainage (Mahfouf and Noilhan 1996), and D (s^{-1}) is the vertical soil moisture diffusion. ρ_w (kgm^{-3}) is the density of liquid water and C_1 is the dimensionless surface force-restore soil transfer

coefficient for moisture (Braud et al. 1993; Giordani et al. 1996). In Eqs. 1 and 2, E_{soil} and E_{transp} (ms^{-1}) represent bare soil evaporation and plant transpiration, respectively (Mahfouf and Noilhan 1991; Noilhan and Mahfouf 1996). Plant transpiration stops when w_2 is below w_{wilt}, corresponding to a matric potential of –150 m.

The infiltration rate, I_r, is computed as the difference between the through-fall rate, P_g, and the surface runoff, Q_s.P_g is the sum of three components: the rainfall not intercepted by the canopy, the snowmelt, S_m (ms^{-1}), from the snow pack, and the dripping, d_r (ms^{-1}), from the interception reservoir, W_r (m), which is calculated as follows:

$$d_r = \max\left(0, \frac{W_r - W_{r\,max}}{\Delta t}\right) \quad (4)$$

where $W_{r\,max}$ represents the maximum amount of water stored within the canopy reservoir and Δt is the model time step. In the original ISBA LSM, the sub-grid surface runoff formulation was introduced by Habets et al. (1999a). This formalism takes into account the sub-grid heterogeneity of surface runoff processes through the use of the variable infiltration capacity (VIC) scheme described by Zhao (1992), Dümenil and Todini (1992) and Wood et al. (1992). The saturated fraction of the grid cell computed by the VIC approach depends on soil moisture, precipitation intensity and a shape parameter. This parameter, which takes a constant and uniform value of 0.5 here, is still poorly known and is generally calibrated in regional applications. In this study, ISBA is used as a global land surface model and has not been tuned for giving particularly good results over the Rhône river basin. A schematic representation of ISBA is shown in Fig. 1.

Note that all force-restore coefficient and soil hydrological parameters are related to soil textural properties (Noilhan and Lacarrére 1995) and moisture using the parameter expressions and values from Clapp and Hornberger (1978). Parameters representing the land surface are calculated by aggregation methods based on the fractional coverage or frequency of occurrence of varying surface types within a grid box assuming that aggregation operators are consistent with the averaging process of the surface fluxes (Noilhan and Lacarrére 1995).

Finally, a new version of ISBA has been recently developed, in which the soil column assumes an exponential profile of the saturated hydraulic conductivity, k_{sat}, with soil depth (Decharme et al. 2005). This parameterization depends only on two parameters, which represent the rate of decline of the k_{sat} profile and the depth where k_{sat} reaches its compacted value. The first parameter takes a constant value of 2 m^{-1} over the entire basin and the second assumes to be equal to rooting depth. Sensitivity tests to these parameters and a detailed discussion about this parameterization can be found in Decharme et al. (2005). The main hypothesis is that roots and organic matter favor the development of macropores and enhance the water movement near the soil surface, and that soil compaction is an obstacle for vertical water transfer in the deeper soil. This exponen-

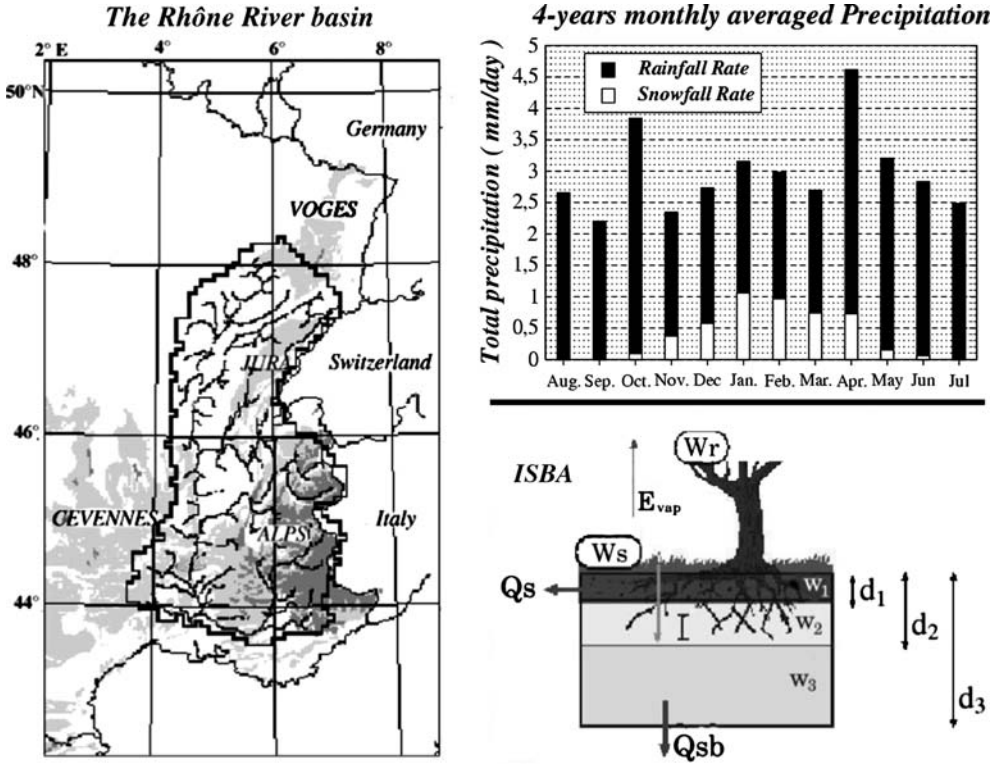

Fig. 1 Representation of the Rhône River basin (*left*), monthly mean basin-average precipitation rate (*right top*) and a schematic representation of the ISBA model (*right bottom*). All variables are defined in Sect. 2

tial soil profile increases the saturated hydraulic conductivity at the surface by approximately a factor of 10, and its mean value increases in the root zone and decreases in the deep layer in comparison with the values given by Clapp and Horneberger (1978).

3 Implementation of a sub-grid hydrology

3.1 Vegetation and soil properties

In recent years, an increasing number of LSMs have adopted the so-called tile approach in which each grid cell is divided into a series of sub-grid patches (Koster and Suarez 1992; Liang et al. 1994; Essery et al. 2003). This method has the advantage of explicitly representing very distinct surface types with specific properties.

The tile approach chosen for representing land cover and soil depth heterogeneities within the ISBA LSM is very simple: each sub-grid patch extends vertically throughout the soil–vegetation–snow column. So, one rooting depth and one soil depth are assigned to each surface class provided by the Rhône-AGG data set (Table 2), and ISBA computes distinct energy and water budgets for each tile within a grid box. Finally, the relative fractional coverage of each surface type within each grid box is used to determine the grid box average of the various output variables.

3.2 Dunne runoff: sub-grid variability of soil moisture

The right partitioning of total runoff into surface runoff (fast runoff component) and drainage (slow runoff component) is a crucial process for the simulation of river discharge (Lohmann et al. 1998; Boone et al. 2004; Decharme et al. 2005) at the hourly to the daily time scale. The first mechanism that produced surface runoff occurs when the soil becomes saturated at the surface from below due to rainfall and/or redistribution of soil moisture. Then, a contributing area grows over the catchment and all the rain that falls on this saturated area generates surface runoff. This saturation mechanism, called Dunne runoff, mainly occurs in humid, vegetated or slightly sloped areas where infiltration capacities of the soil surface are high, relative to normal rainfall intensities.

The sub-grid topography has a strong influence on the generation of soil moisture heterogeneity and runoff. Beven and Kirkby (1979) and Silvapalan et al. (1987) proposed a simple hydrological forecasting model, named TOPMODEL that attempted to combine the important distributed effects of channel network topology and dynamic contributing areas for runoff generation. The coupling between ISBA and TOPMODEL was first introduced by Habets and Saulnier (2001) using the two-layer soil hydrology. Then, it was generalized to the three-layer version of ISBA (Decharme et al. 2005). The TOPMODEL formalism has two main advantages on the VIC sub-grid scheme. First, it takes into account topographic heterogeneities explicitly and secondly, its formulation depends on any calibration (Appendix 1). This formalism permits to determine the fraction, f_{sat}, of each grid cell that is saturated, and thus the Dunne runoff, $Q_{\mathrm{s}}^{\mathrm{D}}$

$$Q_{\mathrm{s}}^{\mathrm{D}}=P_{\mathrm{g}}\times f_{\mathrm{sat}} \tag{5}$$

3.3 Horton runoff: sub-grid variability of infiltration capacity

The second mechanism that produced surface runoff is called Horton runoff and occurs for a rainfall intensity that exceeds the effective maximum infiltration capacity. This infiltration excess mechanism tends to dominate the overland flow production in most desert or semiarid regions where short rainfall events can be very intense, and also where the absence of vegetation and other organic matter prevents the development of a porous soil structure through which water can move easily. The development of a thin crust at the soil surface can also inhibit the infiltration (arid or frozen soil).

The infiltration process depends on the spatial variability of precipitation and soil hydraulic properties. As a first-order approximation, the sub-grid variability in liquid precipitation, P_i, can be given by an exponential probability density distribution, $f(P_i)$ (Entekhabi and Eagleson 1989). The main assumption is generally, that the rainfall intensity is not distributed homogeneously over the entire grid cell. At a low-resolution, a fraction, μ, of a grid cell affected by rainfall can be determined (Appendix 2). The first consequence is that the expression of the dripping (Eq. 4) from the canopy reservoir can be modified according to Mahfouf et al. (1995):

$$d_{\mathrm{r}}=\overline{P}e^{\frac{\mu(W_{\mathrm{r}}-W_{\mathrm{rmax}})}{\overline{P}\Delta t}} \tag{6}$$

where $\overline{P}$ represents the mean rainfall rate over the grid cell.

The second consequence is that the Horton runoff, $Q_{\mathrm{s}}^{\mathrm{H}}$, can be calculated by integrating the difference between the local rainfall and the local maximum infiltration capacity, I_i (Entekhabi and Eagleson 1989) as follows:

$$Q_{\mathrm{s}}^{\mathrm{H}}=\mu\int_{I_i}^{\infty}(P_i-I_i)f(P_i)\,\mathrm{d}P_i \tag{7}$$

Another assumption must be made on the spatial heterogeneity of the local maximum infiltration capacity. Its spatial distribution can also be approximated by an exponential probability density distribution (Yu 2000). The last step is to consider that maximum

infiltration capacity depends on soil freezing. On unfrozen soils, the local maximum infiltration capacity function, as in Chen and Kumar (2001), is given according to Abramopoulos et al. (1988) and Entekhabi and Eagleson (1989). On frozen soils, it is given according to Johnsson and Lundin (1991). The fraction of frozen soil in ISBA can be linked to the amount of ice in a reservoir corresponding in the present study to 50% of the rooting depth. Finally, the total surface runoff can be expressed as follows:

$$Q_s = Q_s^D + (1 - f_{sat})Q_s^H \quad (8)$$

See Appendix 2 for more details about the Horton runoff parameterization.

4 Experimental design

4.1 Brief overview of the Rhône-AGG data set

The Rhône is the largest European river flowing into the Mediterranean Sea. The corresponding basin covers over 95,000 km^2 mostly in southeastern France (Fig. 1). Observed high-resolution soil and vegetation characteristics, subsurface parameters and atmospheric forcing are mapped onto the Rhône domain on 8 km by 8 km grid as part of the GEWEX-Rhône project, which was conceived in recent years by the French research community in order to study the continental water cycle on the regional scale.

The high-resolution Rhône-AGG atmospheric forcing is calculated using the SAFRAN (analysis system for providing atmospheric information relevant to snow) analysis system (Durand et al. 1993). The input atmospheric data consist of standard screen-level observations at approximately 60 Météo-France weather network sites within the domain. The data are counted over 249 homogeneous climatic zones. The total daily precipitation is analyzed using observational data, which comes from over 1,500 gauges, together with a vertical gradient of precipitation (with altitude) derived from climatology. All the forcing variables are available at a 3-hourly time step. Four years of forcing are used in the current study, starting August 1, 1985, and ending July 31, 1989. The 4-year monthly averaged rainfall and snowfall rates are shown in Fig. 1. SAFRAN computes the vertical profile of each atmospheric variable every 6 h within each climatic zone. The parameters are then interpolated to 1-h intervals and to the 8 km by 8 km grid. Further details can be found in Habets et al. (1999b) and Etchevers et al. (2001).

Soil and vegetation data are available at the same resolution as the atmospheric forcing. Soil parameters are defined using the soil textural properties from the INRA (National Institute of Agronomical Research) soil database (King et al. 1995). Vegetation parameters are defined using a vegetation map from the Corine Land Cover Archive and a 2-year satellite archive of the Advanced Very High Resolution Radiometer/Normalized Difference Vegetation Index (AVHRR/NDVI; Champeaux et al. 2000). There are ten distinct surface types considered (Table 2), and the relative fractional coverage of each surface type within each grid box was used to determine average values (Table 1) for the 8 km by 8 km grid boxes.

4.2 The hydrological model

The MODCOU distributed hydrological model is used to convert the surface runoff and the drainage produced by ISBA into river discharge and water table variations (Habets et al. 1999a). The surface runoff is transferred to the river, and the routing from each grid cell is based on isochronous zones using a time step of 1 day. The drainage acts as a source for the water table, which is

Table 1 Land surface parameter values averaged over the entire 8 km by 8 km resolution domain

Variable description	Symbol	Average	Range	Units
Superficial soil depth	d_1	0.01	–	m
Rooting depth	d_2	1.54	(2.00, 1.00)	m
Total soil depth	d_3	2.25	(3.00, 1.00)	m
Clay fraction	X_{clay}	0.22	(0.47, 0.04)	–
Sand fraction	X_{sand}	0.31	(0.89, 0.07)	–
Soil porosity	w_{sat}	0.46	(0.49, 0.40)	$m^3\ m^{-3}$
Field capacity volumetric water content	w_{fc}	0.23	(0.34, 0.15)	$m^3\ m^{-3}$
Wilting point volumetric water content	w_{wilt}	0.17	(0.26, 0.07)	$m^3\ m^{-3}$
Hydraulic conductivity at saturation	k_{sat}	6.75	(181, 1.31)	$\times 10^{-6}\ ms^{-1}$
Matric potential at saturation	ψ_{sat}	−0.39	(−0.61, −0.11)	m
b-parameter	b	6.43	(9.94, 4.05)	–
Snow-free surface albedo	$\backslash' A$	0.17	(0.20, 0.15)	–
Minimum stomatal resistance	$R_{s\ min}$	74.91	(150, 40.0)	s^{-1}
Leaf area index—monthly	LAI	1.93	(4.00, 0.00)	$m^2\ m^{-2}$
Snow-free surface roughness—monthly	z_0	0.29	(1.00, 0.01)	m
Vegetation cover fraction—monthly	veg	0.58	(0.91, 0.00)	–

Uniform hydrological parameters are given by Noilhan and Lacarrére (1995)
The average in space and time is given for parameters with the "-monthly" denotation

Table 2 Land cover types and corresponding fixed or monthly vegetation parameters

Class	Description	$R_{s\ min}$	α	d_2	d_3	$\overline{LAI}$	$\overline{Veg}$	$\overline{z_0}$
1	Crops A	40	0.20	1.5	2.0	2.33	0.71	0.05
2	Mediterranean crops	40	0.20	1.5	2.0	0.58	0.29	0.02
3	Cereals A	40	0.20	1.5	2.0	1.79	0.55	0.04
4	Crops B	40	0.20	1.5	2.0	1.67	0.60	0.04
5	Cereals B	40	0.20	1.5	2.0	1.67	0.54	0.04
6	Crops and grassland	40	0.17	1.0	1.5	1.92	0.65	0.05
7	Grassland	40	0.17	1.0	1.5	2.00	0.65	0.06
8	Coniferous forest	150	0.15	2.0	3.0	2.75	0.73	1.00
9	Rocks	–	0.19	0.0	1.0	0.00	0.00	0.01
10	Deciduous forest	150	0.15	2.0	3.0	1.63	0.48	1.00

The overbar denotes the annual mean for monthly parameters
Symbols are the same as in Table 1

modeled using the diffusivity equations. The version of the MODCOU model used in the present study is slightly different from that used in the Rhône-AGG project. The routing in the river and the relation between the aquifer and the river is computed over the reach for all river gages and not only for the one connected to the aquifer. Note also that all components of the Rhône modeling system (SAFRAN-ISBA-MODCOU) have been developed and calibrated independently.

4.3 Experiments

The ISBA LSM is integrated with a 5-min time step for four consecutive annual cycles, but the first year is treated as a spin-up year. Results are validated over the last 3 years (August 1986 to July 1989). Four simulations are performed and these can be summarized as follows:

- *dt92*: This simulation, performed with the three-layer soil hydrology version of the ISBA LSM, includes only the original VIC parameterization of the surface runoff (Habets et al. 1999a).
- *Top*: The surface runoff is given by the TOPMODEL formalism (Decharme et al. 2005). Only the sub-grid variability of topography, and thus the Dunne runoffs, is taken into account.
- *Top_Hort*: The Horton process is added to the Dunne runoff. The total surface runoff takes into account spatial heterogeneities in topography, precipitation and maximum infiltration capacity.
- *Top_Tiles_Hort*: All sources of sub-grid variability related to topography, precipitation, maximum infiltration capacity, vegetation (or land cover) and soil properties are considered.
- *Top_Tiles_Hort_dec*: Same as before, but with all soil columns assuming an exponential profile of the saturated hydraulic conductivity with depth. The purpose of this last simulation is to investigate the relative impact of the vertical soil physics vs horizontal heterogeneities.

Two kinds of experiments are performed. The first type consists of running ISBA with the various parameterizations presented in Sect. 3 over the high-resolution grid (8 km by 8 km). The range and average of each land surface parameter over the entire domain are shown in Tables 1 and 2. The simulated total runoff is used to drive the MODCOU hydrological model, and the simulated discharges are compared to observed data. One set of observations is used for evaluating the ISBA simulations over the Rhône basin, which consists of daily stream-flow data from 88 river gauges. Only sub-basins where damming does not impact the flow too much are used for the validation (Habets et al. 1999b; Etchevers et al. 2001). The second type of experiment is based on the same design. The only difference is that simulations are performed at a low resolution (1° by 1°) after aggregating all atmospheric forcing and surface parameters. Because the MODCOU model is integrated over the high-resolution grid, the simulated runoff is here linearly disaggregated to the 8 km by 8 km grid before it is transferred to the hydrological model.

5 Results

5.1 High-resolution water budget

The water budget shown in Fig. 2 reveals that the *dt92* and *Top* simulations are very close. Indeed, the partitioning of total precipitation between total runoff and evapotranspiration is approximately 51.5/48.5% for *dt92* against 52/48% for *Top*. Nevertheless, a slight difference appears in the partitioning between surface runoff and drainage. The simulated surface runoff increases slightly with the TOPMODEL formalism (the ratio of surface runoff to total runoff increases from 0.24 for *dt92* to 0.26 for *Top*), while no difference appears in the partitioning of the various evaporative fluxes.

The *Top_Hort* simulation reveals that the inclusion of an exponential distribution of precipitation does not affect, at this resolution, the partitioning of total precipitation between total runoff and evapotranspiration, as well as the evaporative fluxes. As one could expect, the significant impact appears in the partitioning of total runoff between surface runoff and drainage, with the ratio of surface runoff to total runoff increasing from 0.26 for *Top* to 0.36 for *Top_Hort*. The addition of the land cover tiles (*Top_Tiles_Hort*) does not change this ratio but clearly tends to increase the total runoff (53%) to the detriment of evapotranspiration (47%). So, het-

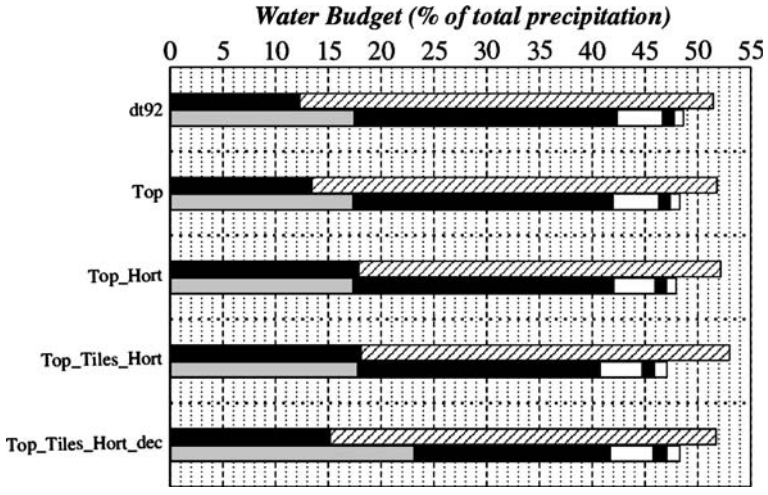

Fig. 2 Comparison of the Rhône basin water budget simulated by each model version at high resolution. The annual mean basin-average ratios of the different hydrological fluxes to total precipitation are represented. For each simulation, the first bar (*top*) corresponds to the runoff components: surface runoff (*solid bar*) and drainage (*dashed bar*). The second bar (*bottom*) corresponds to the evaporative fluxes, from the left to the right: bare soil evaporation (*gray*), plant transpiration (*black*), canopy interception loss (*white*), and ice (*black*) and snow sublimation (*white*)

erogeneities in land cover and soil properties tends to reduce the plant transpiration and favor total runoff.

Finally, the addition of the exponential profile of saturated hydraulic conductivity (*Top_Tiles_Hort_dec*) reduces the total runoff to the benefit of evapotranspiration. This is mainly due to an increase in bare soil evaporation and drainage to the detriment of both surface runoff and plant transpiration. Because average saturated hydraulic conductivity increases in the surface and root zone layer, the influence of the Horton runoff is logically reduced (Eqs. 16a, 16b and 18) compared to a soil with a vertical homogeneous profile. Furthermore, water movements in the root layer are favored. The acceleration of upward and downward flows from this layer to the surface and deep soil leads to a decrease in the rooting zone water content (bare soil evaporation and deep drainage are increased). As a result, the Dunne runoff decreases too (Appendix 1), the deep layer water content increases and drainage is favored (Decharme et al. 2005). Nevertheless, the ratio of surface runoff to total runoff without consideration of the Horton process (but with all others) is near 0.22 (not shown), whereas *Top_Tiles_Hort_dec* has a ratio of 0.29. So, even if the influence of the "Horton" surface runoff is reduced compared to *Top_Tiles_Hort*, it remains important.

5.2 Low-resolution water budget

The low-resolution water budget shown in Fig. 3 reveals that the degradation of the resolution induces an increase in evapotranspiration and a decrease in total runoff compared to the high-resolution water budget (Fig. 2). This result is in consistent with those of most LSMs that participated in the Rhône-AGG project.

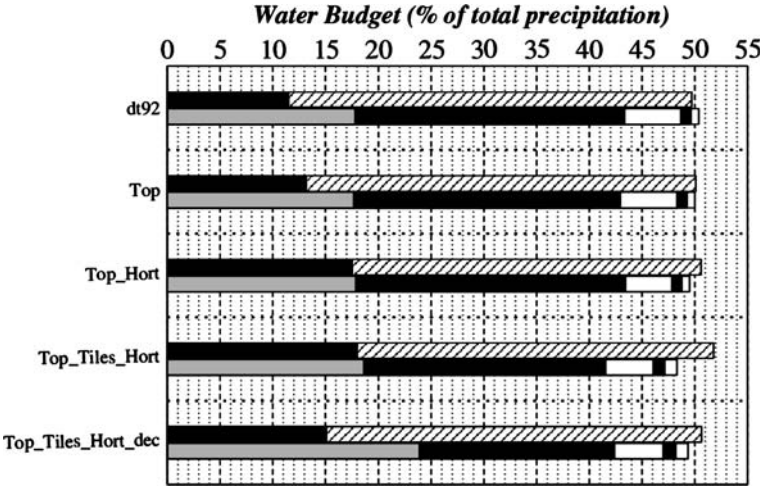

Fig. 3 Comparison of the Rhône basin water budget simulated by each model version at low resolution. Notations are the same as in Fig. 2

The processes that play here a dominant role are now well known. To sum up, the aggregation of vegetation and soil parameters tends to favor plant transpiration instead of total runoff. As shown in Dolman and Blyth (1997), Boone et al. (2004) or Vérant et al. (2004), the dominant effect of the aggregated forcing, particularly of precipitation, is a strong increase in the canopy interception loss during the warm season. Finally, the aggregation of the atmospheric temperature and longwave downward radiation leads to warmer conditions at low resolution, which favors evapotranspiration instead of total runoff. Nevertheless, each additional parameterization tested in the present study (from *dt92* to *Top_Tiles_Hort_dec*) is an attempt to reduce the influence of these sub-grid processes on the simulated water budget.

5.3 Discharges

In this section, the impact of the various parameterizations is analyzed in terms of discharge scores. A global discharge validation based on a daily efficiency comparison (Figs. 4 and 5) is performed with the help of 88 gauging stations distributed over the entire basin. The statistics are shown in Tables 3 and 4 where Eff represents efficiency or Nash–Sutcliffe criteria (Nash and Sutcliffe 1970). In addition, $\overline{R^2}$ and $\overline{Q_{sim}/Q_{obs}}$ represent the square-correlation and ratio between simulated and observed discharge averaged over the 88 gauging stations. Eff measures the skill of the model at capturing the observed variability of the discharges. It is defined as follows:

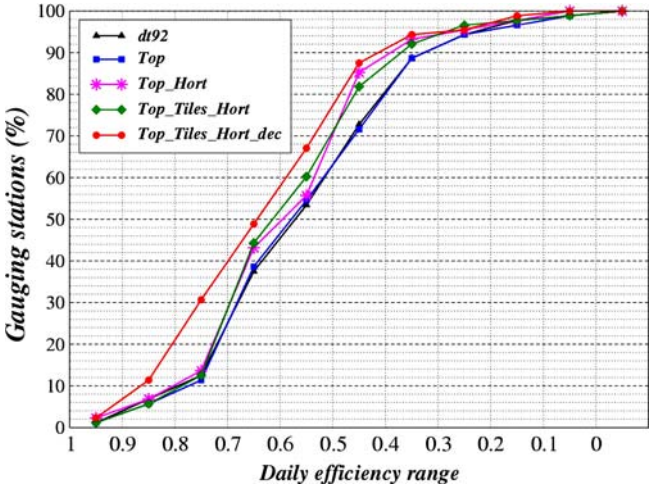

Fig. 4 Cumulative efficiency distributions of daily river discharges simulated at high resolution. These distributions are computed from a dense observation network consisting of daily measurements at 88 gauging stations. Statistics about these distributions are given in Table 3

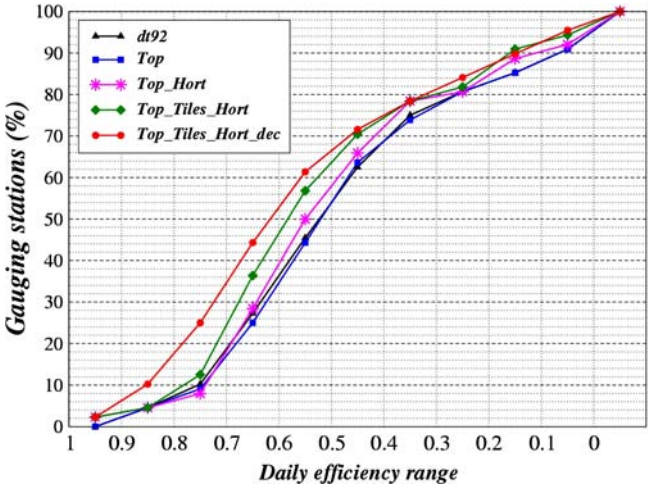

Fig. 5 Cumulative efficiency distributions of daily river discharges simulated at low resolution. Notations are the same as in Fig. 3. Statistics about these distributions are given in Table 4

$$Eff = 1.0 - \frac{\sum_{t=1,N} \left(Q_{sim}(t) - Q_{obs}(t)\right)^2}{\sum_{t=1,N} \left(Q_{sim}(t) - \overline{Q_{obs}}\right)^2}$$

Eff is zero if the model only reproduces the observed temporal mean, $\overline{Q}_{obs}$. It can be negative if the simulated discharge is very poor, is above 0.5 for a reasonable simulation, above 0.7 for a good one and would be 1 for a perfect model (Boone et al. 2004).

As already shown in many studies (Habets and Saulnier 2001; Warrach et al. 2002), the VIC and TOPMODEL approaches are very close, whatever the resolution is. At high resolution, the representation of the sub-grid processes has just a limited influence while the improved hydraulic conductivity has a significant impact on the quality of the simulated discharges (Fig. 3 and Table 3). Nevertheless, this impact is enhanced by the inclusion of the sub-grid variability of soil depth (not shown). The benefit of the various sub-grid hydrological processes is, however, more obvious at the low resolution (Fig. 5) where the mean efficiency calculated over the 88 gauging stations, as well as the mean square correlation (Table 4), is systematically improved by the inclusion of a new sub-grid scheme as well as by the exponential profile of k_{sat}.

5.4 Scaling

The bias calculated between the water budgets simulated at the low and high resolutions (Fig. 6) shows that the model sensitivity to the spatial aggregation is clearly reduced in the *Top_Tile_Hort_dec* experiment, which explains the good discharge scores at low resolution.

The TOPMODEL approach (*Top*) does not improve the results compared to the VIC approach (*dt92*), except for the surface runoff (Q_s) sensitivity. However, the

Table 3 Statistics of the efficiency distribution of the simulated daily river discharges at the high resolution

Simulations	Eff min	Eff mean	Eff max	Eff SD	NSBE	$\overline{R^2}$	$\overline{Q\text{sim}/Q\text{obs}}$
dt92	−0.01	0.52	0.90	0.19	4	0.60	1.02
Top	−0.01	0.52	0.90	0.19	4	0.60	1.03
Top_Hort	0.05	0.54	0.91	0.17	4	0.64	1.04
Top_Tiles_Hort	−0.07	0.54	0.90	0.18	16	0.64	1.05
Top_Tiles_Hort_dec	0.09	0.59	0.92	0.18	60	0.66	1.03

The minimum (min), mean (mean), maximum (max), and standard deviation (SD) of the distribution are shown. The number of stations with the best Eff (NSBE) is also presented. In addition, the mean square correlation ($\overline{R^2}$) and annual ratio of simulated to observed discharges ($\overline{Q\text{sim}/Q\text{obs}}$) over the 88 stations are shown

Table 4 As in Table 3, but for statistics of the efficiency distribution of the simulated daily river discharges at the low resolution

Simulations	*Eff* min	*Eff* mean	*Eff* max	*Eff* SD	NSBE	$\overline{R^2}$	$\overline{Q\text{sim}/Q\text{obs}}$
dt92	−1.58	0.39	0.89	0.36	2	0.55	0.92
Top	−1.50	0.39	0.89	0.35	0	0.55	0.93
Top_Hort	−1.62	0.42	0.91	0.36	1	0.58	0.94
Top_Tiles_Hort	−1.05	0.46	0.91	0.29	24	0.60	0.96
Top_Tiles_Hort_dec	−0.94	0.50	0.92	0.30	61	0.63	0.94

drainage (Q_{sb}) sensitivity is increased. The sub-grid variability of precipitation (*Top_Hort*) reduces the scale dependency of the interception loss (E_{canop}), which is then in better agreement with the dripping simulated at the high resolution. Nevertheless, it leads to a greater sensitivity in plant transpiration (E_{transp}) and bare soil evaporation (E_{soil}), as well as in surface runoff, even if the sensitivity in total runoff ($Q_s + Q_{sb}$) and evapotranspiration (E_{vap}) is slightly reduced.

Including the tiles (*Top_Tiles_Hort*) significantly reduces the sensitivity in plant transpiration, but it slightly enhances that in bare soil evaporation and in interception loss. Nevertheless, the sensitivity in all runoff components and in evapotranspiration is drastically reduced. Finally, the exponential profile of saturated hydraulic conductivity tends to significantly reduce the sensitivity in surface runoff, but to the detriment of that of drainage.

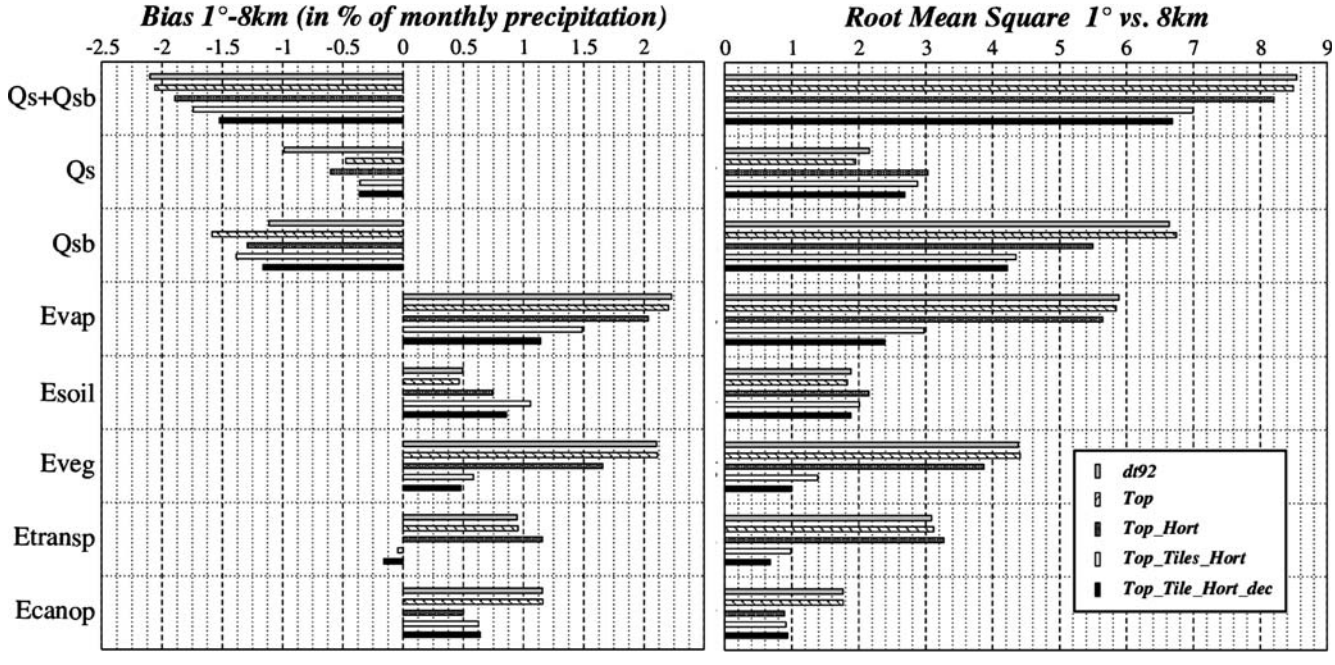

Fig. 6 Impact of scaling on the simulated water budget. The low-resolution experiment (1° by 1°) is compared to the high-resolution experiment (8 km by 8 km). The bias and root mean square are calculated for each surface hydrological fluxes: total runoff ($Q_s + Q_{sb}$), surface runoff (Q_s), drainage (Q_{sb}), evapotranspiration (E_{vap}), bare soil evaporation (E_{soil}), vegetation evapotranspiration (E_{veg}), which is the sum of plant transpiration (E_{transp}) and canopy interception loss (E_{canop}). The bias and root mean square are calculated using the basin-average ratio of each monthly mean flux ($\overline{Flux}_{month}$) to monthly mean precipitation ($\overline{P}_{month}$) in %: $100 \times (\overline{Flux}_{month}/\overline{P}_{month})$. The bias takes into account the absolute difference whereas the root mean square takes into account the monthly difference between both experiments

In summary, the overall benefit of the new parameterizations is that total runoff and evapotranspiration sensitivities to spatial aggregation are clearly reduced. As a result, the new model version shows discharge scores that are less sensitive to spatial resolution (Fig. 7). This is true at least for largest river basins where the model version is much more relevant than the spatial resolution. Conversely, this is not found for the small sub-basins where the main limitation of the scores is the model resolution.

6 Discussion

Describing sub-grid variability of topography through the TOPMODEL formalism has a limited impact on the ISBA simulations compared to the more empirical VIC formalism. Nevertheless, TOPMODEL parameters here only depend on soil properties (Decharme et al. 2005). As a consequence, no calibration is needed whereas the VIC formalism depends on one parameter that is generally calibrated in regional applications. At the global scale, the calibration of this parameter appears as a difficult task implying that the TOPMODEL formalism brings a significant advantage. This formalism has already been tested at the global scale giving a clear improvement compared to the VIC approach of the simulated discharges in many regions of the globe.

In ISBA, the Dunne runoff is estimated through the use of the TOPMODEL formalism whereas the sub-grid variability of rainfall, simply coupled with the spatial heterogeneity in maximum infiltration capacity, permits to calculate the Horton runoff. Its introduction within ISBA has a limited influence on the simulations over the Rhône basin. Nevertheless, the distinction between frozen and unfrozen soil is essential for global scale applications. Indeed, the surface runoff on frozen soil is critical to simulate the discharges of the high latitude rivers. Boone et al. (2004) showed that the impact of upscaling on the Rhône water budget was similar among most LSMs that participated to the Rhône-AGG project, with increased canopy interception loss and decreased runoff. Vérant et al. (2004) showed same results over the Iberian Peninsula. As a consequence, the sub-grid rainfall variability introduced within ISBA (Eq. 5), that significantly reduces both the canopy interception loss and its sensitivity to resolution appears as an important parameterization.

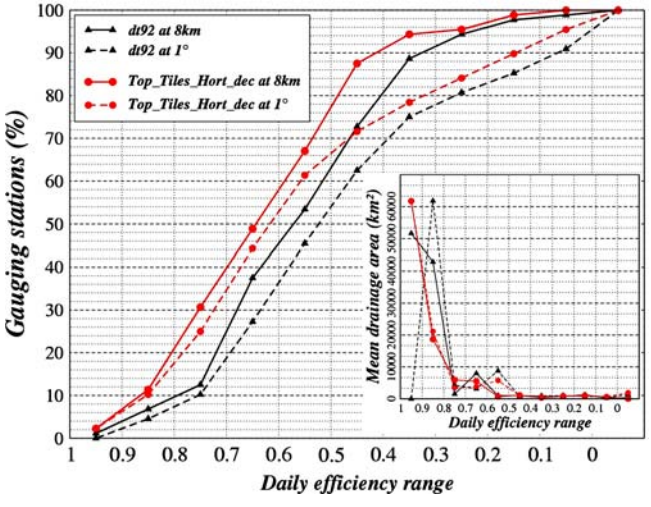

Fig. 7 Impact of scaling on the simulated discharge scores. The same cumulative daily efficiency distributions at high and low resolution of *dt92* and *Top_Tiles_Hort_dec* as in Figs. 3 and 4 are shown. For each experiment, the mean drainage area by efficiency range is also shown (*right bottom*)

The sub-grid hydrological processes linked to the spatial variability of vegetation and soil properties show the most significant impact on the simulations. The scaling sensitivity of plant transpiration is drastically reduced, leading to a better scaling resistance of the model for both evapotranspiration and total runoff. Indeed, at low resolution, more total runoff is produced by ISBA and the discharge quality is improved. Moreover, the positive impact of the exponential profile of saturated hydraulic conductivity is enhanced by the sub-grid variability of soil depth, which also improves the discharge quality at the low resolution. The main disadvantage of the tile approach is an increase in the number of variables and parameters to be stored in memory and in computational cost. This drawback could be important for numerical weather prediction or GCM applications.

At high resolution, the need to include sub-grid hydrological processes appears less important. Nevertheless, the improvement of the simulation due to these sub-grid parameterizations is not negligible. For example, the ISBA version with both the exponential profile of saturated hydraulic conductivity and the TOPMODEL formalism (not shown) reveals a mean efficiency of 0.55 (Decharme et al. 2005) against 0.59 for *Top_Tiles_Hort_dec*. So, the other sources of sub-grid variability, especially land cover and soil depth, remain important even at this scale.

The scope of these conclusions is open to debate since the Rhône river basin is a relatively small region compared to the global domain of application of the ISBA model. Nevertheless, this basin contains a large variety of climate types (Mediterranean in the south, temperate in the north, mountainous in the east and a drier climate in the west). Globally speaking, all additional parameterizations improve the simulated discharges, but some of them appear more useful than other in some regions as, for example, TOPMODEL over the Alpine sub-basins with a strong orography, the Horton runoff in the Southwest and in the North, the vegetation tiles everywhere (except over the Alps where the vegetation is less denser) and the exponential profile of k_{sat} over the North and the Southeast. The scaling sensitivity shows the same spatial characteristics. Indeed, the effect of the sub-grid variability of rainfall dominates over the rainy areas (the Northeast

and the mountains in general), while the impact of the spatial variability of vegetation and soil properties is significant over the whole domain (especially in the South). The exponential profile of k_{sat} has a clear effect in the North, even if this impact is more heterogeneous than for the other parameterizations.

7 Conclusions

This study shows the impact of various parameterizations of sub-grid hydrology on the water budget, simulated over the French Rhône River basin, using the ISBA LSM. These parameterizations account explicitly for the sub-grid variability of topography, precipitation, maximum infiltration capacity, and vegetation and soil properties. All simulations are implemented using both the high- (8 km by 8 km) and low- (1° by 1°) resolution database proposed in the Rhône-AGG project (Boone et al. 2004).

Results show a significant improvement of the simulated daily discharges at the low resolution. Moreover, at the high resolution, the impact of the various sub-grid parameterizations, especially the tile approach, is not negligible. The representation of the sub-grid rainfall distribution decreases the model scaling sensitivity of the interception loss whereas the tiles increase the scaling resistance of plant transpiration and total runoff. As a consequence, the new model version including all sub-grid parameterizations and the exponential profile with depth of saturated hydraulic conductivity significantly improves the quality of the simulated discharges as well as the resistance to the spatial aggregation. Nevertheless, it is important to note that realistic simulations of river discharges do not guarantee realistic simulations of soil moisture. Even with prescribed observed precipitation, a poor simulation of surface evaporation can be associated with a realistic production of runoff, if water storage variations can compensate for the evaporation biases.

The validation of this new version of ISBA at the global scale should be more difficult for at least three reasons. First, the atmospheric forcing and the surface parameters available for this purpose are relatively uncertain compared to the Rhône-AGG data set. The general quality of the hydrological simulations over the Rhône basin is not only due to the robustness of the ISBA physics, but also to the accuracy of the atmospheric forcing derived from the SAFRAN analysis. Secondly, discharge measurements over large river basins are mainly available at a monthly time scale, while the present study emphasizes the relevance of daily observations for a careful validation of regional hydrological simulations. Thirdly, MODCOU is a regional hydrological model that cannot be used for global scale applications so that a more general but simpler river routing model is needed for a global validation. Nevertheless, it will be shown in a future study that this new model version of ISBA also improves many aspects of our hydrological simulations at the global scale.

Acknowledgments The authors thank all their colleagues at the many French laboratories that have participated in the development of the Rhône modeling system (BRGM, CEMAGREF, CEPT, CIG, LTHE, Météo-France/CNRM and CEN). Finally, the authors also wish to thank A. Boone and F. Habets for their useful comments on the Rhône modeling system. Thanks are also due to the anonymous reviewers for their constructive comments. This work was supported by Météo-France/CNRM and by the ACI "Observation de la Terre" of the French Research Ministry.

8 Appendix 1

8.1 Dunne surface runoff formulation

Here, the coupling between ISBA and TOPMODEL is briefly reviewed. More details can be found in Habets and Saulnier (2001) and Decharme et al. (2005). TOPMODEL describes generally the evolution of a water storage deficit near the soil surface. Therefore, the active layer chosen for the ISBA-TOPMODEL coupling is the root layer, and not the total soil column.

The Dunne surface runoff is then simply given by $Q_s^D = P_g \times f_{sat}$ where f_{sat} is the saturated fraction of a grid cell. f_{sat} is inversely proportional to the mean water storage deficit, D_t (m), of a grid cell computed as follows:

$$0 \leq D_t = (w_{sat} - \overline{w_2}) \times \overline{d_2} \leq d_0 \quad (10)$$

$$d_0 = (w_{sat} - w_{wilt}) \times \overline{d_2} \quad (11)$$

where d_0 (m) is the maximum local deficit, and $\overline{w_2}$ and $\overline{d_2}$ are the mean volumetric water contents and depth of the root zone according to the relative fraction of each land surface tiles within each grid cell. In other words, when $\overline{w_2}$ is below the wilting point, the mean water storage deficit is a maximum, $D_t = d_0$, $f_{sat} = 0$ and no surface runoff occurs.

9 Appendix 2

9.1 Horton surface runoff formulation

As previously discussed in Sect. 3, the sub-grid variability in local rainfall, P_i, can be given by an exponential probability density distribution (Entekhabi and Eagleson 1989):

$$f(P_i) = \frac{\mu}{\overline{P}} e^{-\mu(P_i/\overline{P})} \quad (12)$$

where $\overline{P}$ is the mean rainfall rate over the grid cell and μ is the fraction of the grid cell affected by precipitation reaching the surface. μ can be determined using the results of Fan et al. (1996), who showed an exponential relationship between the fractional coverage of precipi-

tation and rainfall rate, based on their analyses of over 2 years radar observations and rain gauge measurements over the Arkansas-Red river basin in the southern plains of the USA. This relationship is:

$$\mu = 1 - \mathrm{e}^{-\beta\overline{P}} \tag{13}$$

where β is a parameter which depends on grid resolution, dx, according to the relationship given by Peters-Lidard et al. (1997):

$$\beta = 0.2 + 0.5\mathrm{e}^{-0.01dx} \tag{14}$$

In Fan et al. (1996), dx represents lengths of square grid cells ranging from 40 to 500 km. In consequence, the μ parameter here is equal to 1 at high resolution because the length of each grid cell is equal to 8 km. At low resolution, it is calculated according to Fan et al. (1996) (Eq. 13), where the β parameter depends, for each grid cell, on the root-square of the grid cell area in km^2 (Eq. 14).

The spatial heterogeneity of the local maximum infiltration rates, I_i, can also be approximated by an exponential probability density distribution (Yu 2000):

$$g(I_i) = \frac{1}{\overline{I}}\mathrm{e}^{-I_i/\overline{I}} \tag{15}$$

where $\overline{I}$ is the mean maximum infiltration rate over the grid cell. Distinction has been made between infiltration on unfrozen and frozen soil. The local maximum infiltration rates on unfrozen soil, I_{unf}, i, is given as in Chen and Kumar (2001) according to Abramopoulos et al. (1988) and Entekhabi and Eagleson (1989), and on frozen soil, I_{f},i, by Johnsson and Lundin (1991). Generalization of these functions into the ISBA framework leads to:

$$I_{\mathrm{unf},\,i} = k_{\mathrm{sat},\,i}\left[\frac{b\psi_{\mathrm{sat}}}{\Delta z}\left(\frac{w_2}{w^*_{\mathrm{sat}}} - 1\right) + 1\right] \tag{16a}$$

$$I_{\mathrm{f},\,i} = k^{\mathrm{ice}}_{\mathrm{sat},\,i}\left(\frac{w_2}{w^*_{\mathrm{sat}}}\right)^{2b+3} \times 10^{-6\frac{w_{I2}}{w_{I2}+w_2}} \tag{16b}$$

where $k_{\mathrm{sat},i}$ (ms^{-1}) is the local surface saturated hydraulic conductivity, ψ_{sat} (m) is the saturated soil water potential or air entry potential, Δz is a soil thickness of 0.1 m, and b is a dimensionless slope parameter (Brooks and Corey 1966; Clapp and Hornberger 1978). w_{12} is the layer-average volumetric ice content (m^3 m^{-3}) in the root zone and w^*_{sat} is the soil porosity in presence of soil ice (Boone et al. 2000). $k^{\mathrm{ice}}_{\mathrm{sat,i}}$ is the local layer-average saturated hydraulic conductivity over a diagnostic reservoir, corresponding to the ice depth, d_{ice}, where the ice can be present. In this study, d_{ice} is equal to 50% of the rooting depth. This calibration gives the best results over the Rhône basin even if Johnsson and Lundin (1991) recommended a value of 0.2 m, which is used at the global scale. Finally, the fraction of the frozen soil in ISBA is given by $\delta_{\mathrm{f}} = \min(w_{I2}\cdot d_2/(w_{\mathrm{sat}}\cdot d_{\mathrm{ice}}), 1)$.

According to Eq. 7, a new expression of the Horton runoff, $Q^{\mathrm{H}}_{\mathrm{s}}$, is given by:

$$Q^{\mathrm{H}}_{\mathrm{s}} = \mu\left[(1-\delta_{\mathrm{f}})\int_0^{\infty}\int_{I_{\mathrm{unf},i}}^{\infty}\left(P_i - I_{\mathrm{unf},\,i}\right)f(P_i)g\left(I_{\mathrm{unf},\,i}\right)\mathrm{d}P_i\,\mathrm{d}I_{\mathrm{unf},\,i} + \delta_{\mathrm{f}}\int_0^{\infty}\int_{I_{\mathrm{f},i}}^{\infty}\left(P_i - I_{\mathrm{f},\,i}\right)f(P_i)g\left(I_{\mathrm{f},\,i}\right)\mathrm{d}P_i\,\mathrm{d}I_{\mathrm{f},\,i}\right] \tag{17}$$

where the first term corresponds to the Horton runoff on unfrozen soil and the second to the Horton runoff on frozen soil. Consequently and passing throughout several algebraic steps, the Horton runoff in ISBA is computed as follows:

$$Q^{\mathrm{H}}_{\mathrm{s}} = (1-\delta_{\mathrm{f}})\frac{\overline{P}}{1+\overline{I_{\mathrm{unf}}}\frac{\mu}{\overline{P}}} + \delta_{\mathrm{f}}\frac{\overline{P}}{1+\overline{I_{\mathrm{f}}}\frac{\mu}{\overline{P}}} \tag{18}$$

where $\overline{I_{\mathrm{f}}}$ and $\overline{I_{\mathrm{unf}}}$ are the grid-average frozen and unfrozen maximum infiltration capacity, respectively. Finally, in the presence of snowmelt, S_{m}, any assumptions about its spatial variability can be made, and the Horton runoff is simply given by:

$$Q^{\mathrm{H}}_{\mathrm{s}} = (1-\delta_{\mathrm{f}})\max\left(0,\, S_{\mathrm{m}} - \overline{I_{\mathrm{unf}}}\right) + \delta_{\mathrm{f}}\max\left(0,\, S_{\mathrm{m}} - \overline{I_{\mathrm{f}}}\right) \tag{19}$$

References

Abramopoulos F, Rosenzweig C, Choudhury B (1988) Improved ground hydrology calculation for global climate models (GCMs): soil water movement and evapotranspiration. J Clim 1:921–941

Beven KJ, Kirkby MJ (1979) A physically based variable contributing area model of basin hydrology. Hydrol Sci Bull 24:43–69

Boone A et al (2004) The Rhône-Aggregation land surface scheme intercomparison project: an overview. J Clim 17:187–208

Boone A, Calvet JC, Noilhan J (1999) Inclusion of a third soil layer in a land surface scheme using the force-restore method. J Appl Meteorol 38:1611–1630

Boone A, Masson V, Meyers T, Noilhan J (2000) The influence of the inclusion of soil freezing on simulation by a soil–atmosphere-transfer scheme. J Appl Meteorol 9:1544–1569

Braud I, Noilhan J, Bessemoulin P, Mascart P, Haverkamp R, Vauclin M (1993) Baregroung surface heat and water exchanges under dry conditions: observation and parameterization. Bound-Layer Meteorol 66:173–200

Brooks RH, Corey AT (1966) Properties of porous media affecting fluid flow. J Irrig Drain Am Soc Civil Eng 17:187–208

Champeaux JL, Acros D, Bazile E, Giard D, Gourtorbe JP, Habets F, Noilhan J, Roujean JL (2000) AVHRR-derived vegetation mapping over western Europe for use in numerical weather prediction models. Int J Remote Sens 21:1183–1199

Chapelon N, Douville H, Kosuth P, Oki T (2002) Off-line simulation of the Amazon water balance: a sensitivity study with implications for GSWP. Clim Dyn 19:141–154

Chen J, Kumar P (2001) Topographic influence on the seasonal and interannual variation of water and energy balance of basin in North America. J Clim 14:1989–2014

Clapp R, Hornberger G (1978) Empirical equations for some soil hydraulic properties. Water Resour Res 14:601–604

Deardorff JW (1977) A parametrization of ground-surface moisture content for use in atmospheric prediction model. J Appl Meteorol 16:1182–1185

Deardorff JW (1978) Efficient prediction of ground surface temperature and moisture with inclusion of a layer of vegetation. J Geophys Res 20:1889–1903

Decharme B, Douville H, Boone A, Habets F, Noilhan J (2005) Impact of an exponential profile of saturated hydraulic conductivity within the ISBA LSM: simulations over the Rhône basin. J Hydrometeorol (in press)

Dirmeyer PA, Dolman AJ, Sato N (1999) The global soil wetness project: a pilot project for global land surface modeling and validation. Bull Am Meteorol Soc 80:851–878

Dolman AJ, Blyth EM (1997) Patch scale aggregation of heterogeneous land surface cover for mesoscale meteorological models. J Hydrol 190:252–268

Douville H (2003) Assessing the influence of soil moisture on seasonal climate variability with AGCMs. J Hydrometeorol 4:1044–1066

Douville H, Royer JF, Mahfouf JF (1995) A new snow parameterization for the Météo-France climate model. Part I: validation in stand-alone experiments. Clim Dyn 12:21–35

Douville H, Chauvin F, Planton S, Royer JF, Salas-Mélia D, Tyteca S (2002) Sensitivity of the hydrological cycle to increasing amounts of greenhouse gases and aerosols. Clim Dyn 20:45–68

Ducharne A, Golaz C, Leblois E, Laval K, Polcher J, Ledoux E, de Marsily G (2003) Development of a high resolution runoff routing model, calibration and application to assess runoff from the LMD GCM. J Hydrol 280:207–228

Dümenil L, Todini E (1992) A rainfall-runoff scheme for use in the Hamburg climate model. Adv Theor Hydrol 9:129–157

Durand Y, Brun E, Méridol L, Guyomarc'h G, Lesaffre B, Martin E (1993) A meteorological estimation of relevant parameters for snow schemes used with atmospheric models. Ann Glaciol 18:65–71

Entekhabi D, Eagleson PS (1989) Land surface hydrology parameterization for atmospheric general circulation models including sub-grid spatial variability. J Clim 2:816–831

Essery RL, Best MJ, Betts A, Cox PM, Taylor CM (2003) Explicit representation of sub-grid heterogeneity in a GCM land surface scheme. J Hydrometeorol 4:530–543

Etchevers P, Colaz C, Habets F (2001) Simulation of the water budget and the rivers flows of the Rhône basin from 1981 to 1994. J Hydrol 244:60–85

Fan Y, Wood EF, Baeck ML, Smith JA (1996) The fractional coverage of rainfall over a grid: analyses of NEXRAD data over the southern plains. Water Resour Res 32:2787–2802

Giordani H, Noilhan J, Lacarrére P, Bessemoulin P (1996) Modeling the surface processes and the atmopheric boundary layer for semi-arid conditions. Agric For Meteorol 80:263–287

Habets F, Saulnier GM (2001) Sub-grid runoff parameterization. Phys Chem Earth 26:455–459

Habets F, Noilhan J, Golaz C, Goutorbe JP, Lacarrére P, Leblois E, Ledoux E, Martin E, Ottlé C, Vidal-madjar D (1999a) The ISBA surface scheme in a macroscale hydrological model applied to the HAPEX-MOBILHY area. Part I: model and database. J Hydrol 217:75–96

Habets F, Etchevers P, Golaz C, Leblois E, Ledoux E, Martin E, Noilhan J, Ottlé C (1999b) Simulation of the water budget and the river flows of the Rhône basin. J Geophys Res 104:31145–31172

Habets F, LeMoigne P, Noilhan J (2004) On the utility of operational precipitation forecasts to serve as input for streamflow forecasting. J Hydrol 293:270–288

Johnsson H, Lundin LC (1991) Surface runoff and soil water percolation as affected by snow and soil frost. J Hydrol 122:141–159

King D, Lebas C, Jamagne M, Hardy R, Draoussin J (1995) Base de données géographiques des sols de France à l'échelle 1/1000000 (Geographical Soil Database for France at a scale of 1/1000000). Institut National de Recherches Agronomiques (INRA) Tech. Rep., Orléans, France, 100pp

Koster DR, Suarez MJ (1992) Modeling the land surface boundary in climate models as a composite of independent vegetation stands. J Geophys Res 97:2697–2715

Liang X, Lettenmaier DP, Wood EF, Burges SJ (1994) A simple hydrologically based model of land surface water and energy fluxes for general circulation models. J Geophys Res 99:14415–14428

Lohmann D et al (1998) The Project for Intercomparison of Land-Surface Parameterization Schemes (PILPS) Phase-2c Red-Arkansas River Basin experiment: III. Spatial and temporal analysis of water fluxes. Global Planet Change 19:161–180

Mahfouf JF, Noilhan J (1991) Comparative study of various formulations of evaporation from bare soil using in situ data. J Appl Meteorol 9:351–362

Mahfouf JF, Noilhan J (1996) Inclusion of gravitational drainage in a land surface scheme based on the force-restore method. J Appl Meteorol 35:987–992

Mahfouf JF, Manzi AO, Noilhan J, Giordani H, Déqué M (1995) The land surface scheme ISBA within the Météo-France climate ARPEGE. Part I: implementation and preliminary results. J Clim 8:2039–2057

Manabe S (1969) Climate and ocean circulation 1. The atmospheric circulation and the hydrology of the earth's surface. Mon Weather Rev 97:739–805

Nash JE, Sutcliffe JV (1970) River flow forecasting through conceptual models: 1. A discussion of principles. J Hydrol 10:282–290

Noilhan J, Lacarrére P (1995) GCM gridscale evaporation from mesoscale modeling. J Clim 8:206–223

Noilhan J, Mahfouf JF (1996) The ISBA land surface parametrization scheme. Global Planet Change 13:145–159

Noilhan J, Planton S (1989) A simple parameterization of land surface processes for meteorological models. Mon Weather Rev 117:536–549

Oki T, Nishimura T, Dirmeyer P (1999) Assessment of annual runoff from land surface models using Total Runoff Integreting Pathways (TRIP). J Meteorol Soc Jpn 77:235–255

Peters-Lidard CD, Zion MS, Wood EF (1997) A soil–vegetation–atmosphere transfer scheme for modeling spatially variable water and energy balance processes. J Geophys Res 102:4303–4324

Seufert G, Gross P, Simmer C, Wood EF (2002) The influence of hydrologic modeling on the predicted local weather: two-way coupling of a mesoscale weather prediction model and a land surface hydrologic model. J Hydrometeorol 3:505–523

Silvapalan M, Beven KJ, Wood EF (1987) On hydrologic similarity: 2. A scaled model of storm runoff production. Water Resour Res 23:2266–2278

Vérant S, Laval K, Polcher J, De Castro M (2004) Sensitivity of the continental hydrological cycle to the spatial resolution over the Iberian peninsulia. J Hydrometeorol 5:267–285

Wolock DM, McCabe GJ (2000) Differences in topographic characteristics computed from 100- and 1,000-m resolution digital elevation model data. Hydrol Process 14:987–1002

Wood EF et al (1998) The Project for Intercomparison of Land-Surface Parameterization Schemes (PILPS) Phase-2c Red-Arkansas River Basin experiment: I. Experiment description and summary intercomparisons. Global Planet Change 19:115–135

Wood EF, Lettenmaier DP, Zartarian VG (1992) A land-surface hydrology parameterization with sub-grid variability for general circulation models. J Geophys Res 97:2717–2728

Yang ZL, Niu GY (2003) The versatile integrator of surface atmospheric processes (VISA) Part 1: model description. Global Planet Change 38:175–189

Yu Z (2003) Assessing the response of sub-grid hydrologic processes to atmospheric forcing with a hydrologic model system. Global Planet Change 25:1–17

Zhao RJ (1992) The Xinanjiang model applied in China. J Hydrol 134:317–381